Dyes and Pigments 133 (2016) 73–78

Contents lists available at ScienceDirect

Dyes and Pigments

journal homepage: www.elsevier.com/locate/dyepig

Colorimetric polarity chemosensor based on a organometal halide perovskite functional dye

Jong H. Kim [a, b], Sung-Hoon Kim [c, *]

[a] Department of Chemical Engineering Education, Chungnam National University, 99 Daehak-ro, Yuseong-gu, Daejeon, 305-764, South Korea
[b] Graduate School of Energy Science and Technology, Chungnam National University, 99 Daehak-ro, Yuseong-gu, Daejeon, 305-764, South Korea
[c] Department of Textile System Engineering, Kyungpook National University, Daegu, 702-701, South Korea

ARTICLE INFO

Article history:
Received 11 April 2016
Received in revised form
24 May 2016
Accepted 25 May 2016
Available online 26 May 2016

Keywords:
Functional dye
Perovskite
Solvent polarity
Chemosensor
Hydrogen bonding

ABSTRACT

We have investigated polarity sensing of organometal halide $CH_3NH_3PbI_3$ perovskite functional dye based on hydrogen bonds between alcohols and polar units in perovskite. Upon exposure of alcohol solvents, perovskite film showed a drastic visible color change with different changing time depending on the polarities of alcohols. From the kinetic study of the reaction between perovskite dye and alcohols having different polarities, efficiency of hydrogen-bonding interactions between them were clearly revealed to be the main sensing mechanism, which enables effective discrimination of polarities by naked eyes. This study suggests a novel and practical sensing platform for highly sensitive colorimetric polarity chemosensors.

1. Introduction

Chemosensors are sensory receptor molecules that are capable of selective detection of interested analytes or chemical properties of interest with a measureable optoelectronic changes. Due to their simplicity, high sensitivity, and real-time detection for various analytes, chemosensors have attracted considerable attention during the past decade [1]. Among them, development of chemosensor systems that have precise and rapid recognizability of polarity of chemical compounds is of particular importance in the chemistry field because most chemical reactions and processes are significantly influenced by polarity of reactant molecules. In particular, choice of organic solvents with appropriate polarity values plays a critical role in organic synthesis, recrystallization, and chromatographic separation of compounds.

Recently, a large number of chemosensors detecting environmentally harmful volatile organic compounds (VOCs), biologically important anions, cations, acidity, and explosive or hazardous chemicals have been extensively developed [2]. Polarity-sensitive probes also have been reported, however, most of their detection mechanisms have been focused on fluorescence emission changes rather than reflective color shifts, and there still remain technical challenges to overcome, such as limitations in marked color/emission wavelengths shifts enough to detect with naked eyes [3]. Even worse, chemosensors or sensing techniques for discriminating molecules having minute polarity differences by displaying distinct outputs color changes are rarely explored. One of the reasons for this research scarcity in the polarity-analyzing system lies in the lack of suitable probing materials satisfying two essential issues for the investigation; i) spontaneous interaction with polar analytes at a molecular level and ii) quick and drastic visible color conversion after detection.

Organometal halide-type hybrid perovskites with a structure of ABX_3 (A = organic cation, B = metal cation, and X = halogen anion) have emerged as a new functional dye due to their unprecedented optoelectronic properties such as intense broad-band UV/Vis light absorption (300–800 nm) and 10 times greater absorption coefficient ($\varepsilon = 1.3 \times 10^5$ cm^{-1} at 550 nm) compared to that of the conventional light-absorbing ruthenium-based molecular dye [4]. Moreover, as shown in Fig. 1a, ionic interactions between the organic and inorganic portions in the structure of this hybrid perovskite dye, for example $CH_3NH_3PbI_3$, facilitate its sensitive interactions with polar molecules. This unique character allows spontaneous crystal structure conversion into CH_3NH_3I and PbI_2 in response to polar environments concomitant with a fast and

---

* Corresponding author.
E-mail address: shokim@knu.ac.kr (S.-H. Kim).

http://dx.doi.org/10.1016/j.dyepig.2016.05.049
0143-7208/

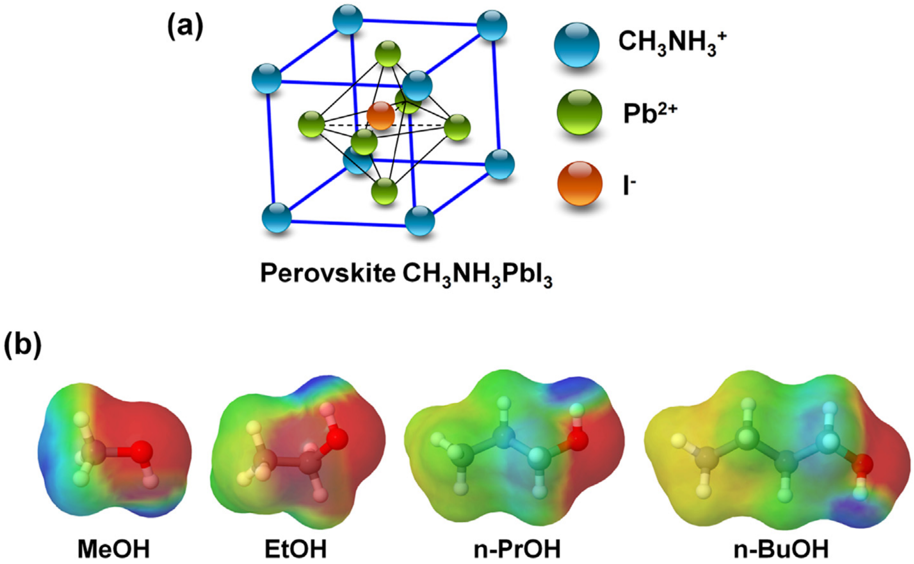

Fig. 1. (a) General (ABX_3) crystal structure of organometal halide perovskite ($CH_3NH_3PbI_3$). (b) Molecular electrostatic potential surface diagrams of MeOH, EtOH, n-PrOH, and n-BuOH.

discernible color conversion, according to the following chemical equation [5].

$$CH_3NH_3PbI_3 \rightarrow CH_3NH_3I + PbI_2 \quad (1)$$

Taking advantages of these satisfactory optical and chemical properties which are compatible with the investigation on the molecule's polarity, herein, we introduced $CH_3NH_3PbI_3$ perovskite dye as a polarity sensing probe in attempt to develop an effective colorimetric polarity chemodosimeter. We demonstrate a simple but very effective method to distinguish polarities of alcohol solvents with minute difference in polarity values. The differences in optical responses and kinetics of hydrogen bonding interactions between perovskite and alcohols with different polarity provide insights into the photophysical polarity-sensing mechanism of perovskite.

2. Experimental section

2.1. Materials

Chemical reagents used in this study were used without any further purification. Methylammonium iodide (CH_3NH_3I) and lead (II) iodide (PbI_2) were purchased from Tokyo Chemical Industry (TCI). Dimethyl sulfoxide (DMSO), methanol (MeOH), ethanol (EtOH), n-propanol (n-PrOH), and n-butanol (n-BuOH) were purchased from Sigma-Aldrich.

2.2. Film preparation and characterization

$CH_3NH_3PbI_3$ perovskite precursor solution was prepared using CH_3NH_3I and PbI_2 following the reported method [6], and the perovskite films in this study were prepared on the glass substrates. The substrates were rinsed by sonication in detergent and deionized water, acetone and isopropyl alcohol before film coating. Then, uniform and large-area (10 cm^2) perovskite films were prepared in ambient condition by using a blade-coater and homogeneous $CH_3NH_3PbI_3$ precursor solution in DMSO. The wet films formed immediately after solution blading were kept at room temperature for 40 min before annealing to wait for the majority of DMSO solvent to be dried and evaporated. Finally, the substrates were annealed at 100 °C for 15 min to complete perovskite film fabrication. ~400 nm-thick perovskite layers were obtained by blade-coating the precursor solution with a coating speed of 10 mm/s with the gap between blade and substrate of 10 μm at room temperature (Blade-coating was performed using a knife-coating device (KP-3000H, KIPAE). UV–vis absorption spectra were obtained using an Agilent 8457 UV–vis spectrophotometer. X-ray diffraction (XRD) data were recorded using a Rigaku D/max-2500 diffractometer. Electrostatic potential surface of alcohols were calculated using Avogadro and Jmol softwares.

3. Results and discussion

The crystal structure of perovskite dye ($CH_3NH_3PbI_3$) used in this study can be described by the general formula ABX_3, as shown in Fig. 1a. These organic-inorganic hybrid crystals are fixed together by the interaction between organic cation ($CH_3NH_3^+$) and inorganic anion (PbI_3^-) component through hydrogen bonds between the hydrogens on the NH_3^+ and the iodide atoms ($N-H/I^-$) and the hydrogens on the CH_3 and iodide atoms ($C-H/I^-$) [4].

We prepared $CH_3NH_3PbI_3$ films using mixed precursor (CH_3NH_3I/PbI_2 in DMSO) solution using a blade-coating method, which is convenient and effective technique for large-area printing. The wet films deposited by a blade-coater were dried under room-temperature before annealing for crystallization at 100 °C. Formation of $CH_3NH_3PbI_3$ from wet film to the crystallized structure was clearly confirmed from the gradual evolution of absorption spectra and film color changes as shown in Fig. 2.

Firstly, to demonstrate the potential applications of $CH_3NH_3PbI_3$ perovskite films to colorimetric probes for the polarity detection of organic molecules, absorption spectral studies of $CH_3NH_3PbI_3$ film in the presence of alcohol solvents with different polarities were performed. For this study, the time course of the reaction between $CH_3NH_3PbI_3$ film and EtOH was investigated by monitoring the absorption intensities of the $CH_3NH_3PbI_3$ at λ_{max} (420 nm). As shown in Fig. 3, it was observed that strong intensity of absorption band at 420 nm quickly decreased to 60.2% of its initial one in less than 5 min, accompanied by a significant color changes from dark brown to yellow, with exposure to the EtOH solvent.

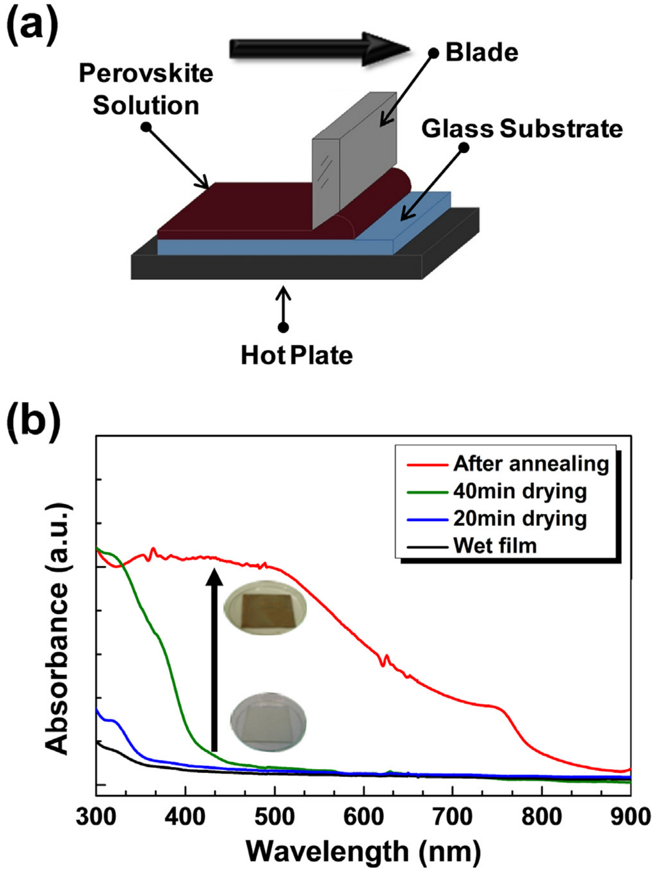

Fig. 2. (a) Schematic diagram of blade-coating process. (b) Evolution of UV/Vis absorption spectra from bladed wet film to annealed crystallized film.

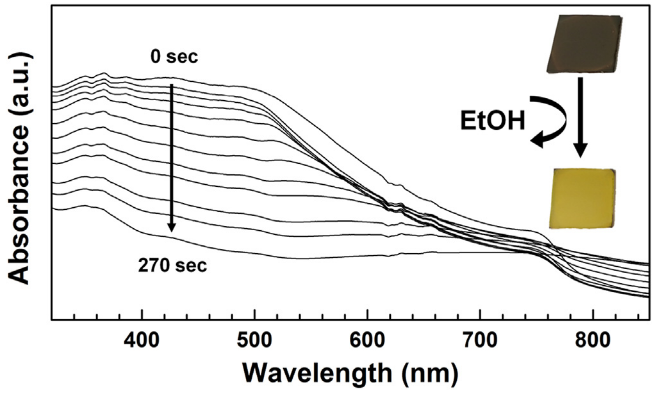

Fig. 3. UV/Vis absorption spectra change of $CH_3NH_3PbI_3$ upon exposure to the EtOH with time (0–270 s).

After then X-ray diffraction (XRD) measurements were performed on the $CH_3NH_3PbI_3$ film in order to investigate the origin of these color changes. Fig. 4 compares XRD spectra of $CH_3NH_3PbI_3$ perovskite films before and after EtOH exposure. Before exposure, the film shows intense XRD peaks corresponding to crystalline perovskite at $2\theta = 14.08$ and $28.38°$, assigned to (110) and (220) planes of the $CH_3NH_3PbI_3$ crystal, indicating an orthorhombic crystal structure of organometal halide perovkskite [7]. However, after 5 min exposure to EtOH solvent, the XRD peaks from perovskite crystal totally disappeared, and we observed a new strong signal at $2\theta = 12.63°$ which can be assigned to the (001) diffraction peak of PbI_2 [8]. These results reveal that the color or absorption spectral changes originated from the structural conversion of $CH_3NH_3PbI_3$ into PbI_2, which responds very sensitively to polar EtOH exposure.

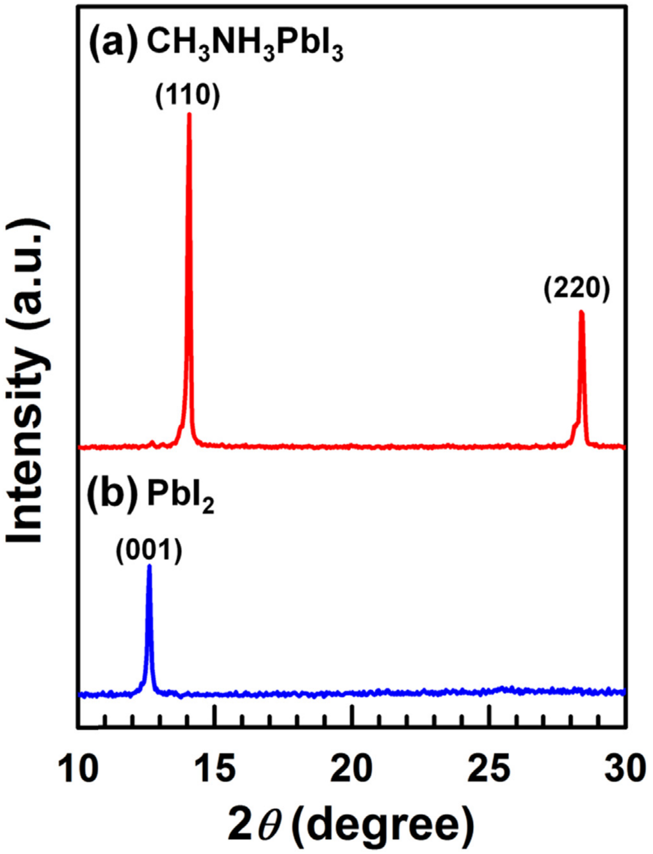

Fig. 4. XRD patterns of (a) a pristine $CH_3NH_3PbI_3$ film and (b) a $CH_3NH_3PbI_3$ film after 5 min exposure to EtOH.

It has been reported that $CH_3NH_3PbI_3$ makes complexes with polar species such as H_2O by forming both monohydrate $CH_3NH_3PbI_3{\cdot}H_2O$ and dihydrate $(CH_3NH_3)_4PbI_6{\cdot}2H_2O$ following the reaction below.

$$4CH_3NH_3PbI_3 + 4H_2O \leftrightarrow 4[CH_3NH_3PbI_3{\cdot}H_2O] \leftrightarrow (CH_3NH_3)_4PbI_6{\cdot}2H_2O + 3PbI_2 + 2H_2O \quad (2)$$

The main driving force of this hydration (moisture intercalation into the perovskite lattice) is the formation of hydrogen bonding interaction between the hydrogen atoms of the H_2O and the iodide atoms ($O{-}H/I^-$), and that between the oxygen atoms of the H_2O and the hydrogen atoms of NH_3^+ ($N{-}H/O$). Based on the same principle, polar alcohols containing OH group will form similar types of hydrogen bonding interactions with $CH_3NH_3PbI_3$ perovskite crystal lattices (Fig. 5 shows the proposed mechanism of perovskite crystal structure conversion via hydrogen bonding interactions between EtOH and ionic components of the $CH_3NH_3PbI_3$ ($O{-}H/I^-$, $N{-}H/O$)) [9].

Furthermore, according to the theoretical calculation, the stabilization energy of the $N{-}H/O$ hydrogen bond is much stronger than those of the $N{-}H/I^-$ and $C{-}H/I^-$ in the $CH_3NH_3PbI_3$ [10]. This evidence supports that new hydrogen bonds between $CH_3NH_3^+$ and alcohols are much stronger than those between $CH_3NH_3^+$ and PbI_3^-, which leads to the conversion of crystal structure and absorption spectra changes, and consequently the drastic visible color changes

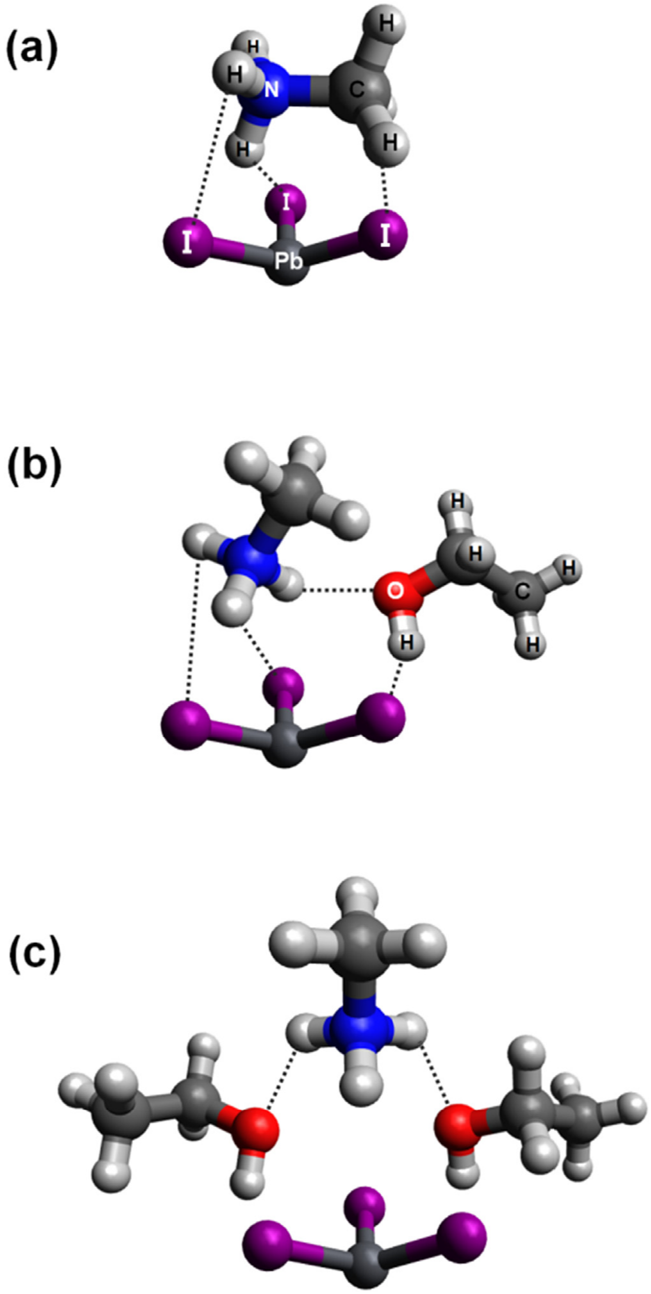

Fig. 5. Hydrogen bonding interactions (a) between $CH_3NH_3^+$ and PbI_3^- in $CH_3NH_3PbI_3$, (b) between $CH_3NH_3PbI_3$ and one EtOH molecule, and (c) between $CH_3NH_3PbI_3$ and two EtOH molecules.

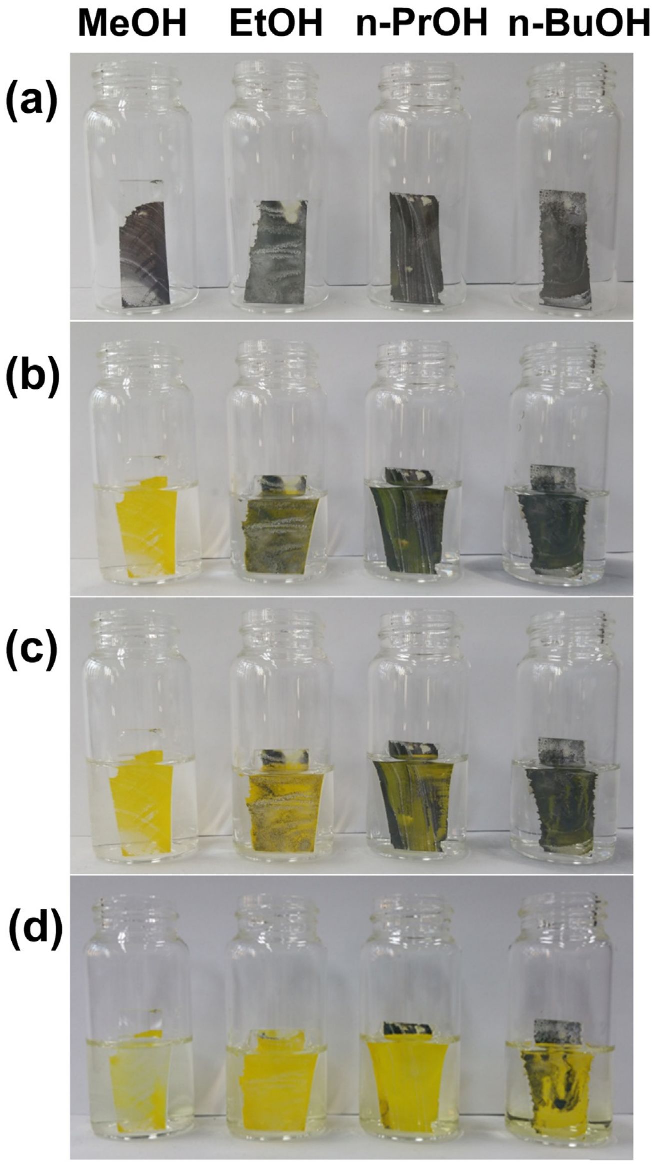

Fig. 6. Photographs showing the different time ((a): 0, (b): 5 min, (c): 15 min, and (d): 30 min) for visible color shifts of the $CH_3NH_3PbI_3$ films depending on the exposed alcohols.

of perovskite films after EtOH exposure.

Motivated by this excellent perovskite's reactivity with polar molecules accompanied by sensitive optical signal changes, we have turned our attention to $CH_3NH_3PbI_3$ for the application of colorimetric polarity sensors for four different alcohols (MeOH, EtOH, n-PrOH, and n-BuOH).

$CH_3NH_3PbI_3$ perovskite films exhibit clear color change from dark brown to yellow in response to the exposure of four alcohol solvents. We recorded photographs at regular intervals (i.e., 0, 1, 10, and 30 min) as shown in Fig. 6. Interestingly, each sample shows noticeable difference in color conversion time depending on the kinds of alcohols with different polarities (E_T) or dipole moments (μ). Most polar alcohol, MeOH ($E_T = 55.4$ kcal mol^{-1}, $\mu = 1.70$ D) exhibited rapid color conversion in 2 min, while elapsed time for n-BuOH, relatively less polar alcohol ($E_T = 50.2$ kcal mol^{-1}, $\mu = 1.63$ D), was 30 min. Based on these observations we could infer that minute difference in polarity values significantly influences hydrogen bonding interaction between $CH_3NH_3PbI_3$ and alcohols (dielectric constant, polarity and dipole moment values of MeOH, EtOH, n-PrOH, and n-BuOH are summarized in Table 1).

In order to further understand the recognition of $CH_3NH_3PbI_3$ towards alcohol's polarity, we examined the kinetic profiles of the $CH_3NH_3PbI_3$ perovskite's reaction under first-order reaction with four different alcohols (MeOH, EtOH, n-PrOH, and n-BuOH). The first-order rate constant (k) can be calculated according to the following equation:

$$\ln(A_t - A_\infty)/(A_i - A_\infty) = kt \tag{3}$$

where A_i is the absorbance at 420 nm, and A_t is the absorbance at 420 nm at time t after exposure to the alcohol. A_∞ and k refer to

Table 1
Summarized physical characteristics of alcohols (polarity, dielectric constant, dipole moment, rate constant).

Alcohol	Polarity (E_T, kcal/mol)	Dielectric constant	Dipole moment (μ, D)	k (sec^{-1})
MeOH	55.4	33	1.70	1.13×10^{-1}
EtOH	51.9	30	1.69	9.78×10^{-3}
n-PrOH	50.7	20	1.68	1.14×10^{-3}
n-BuOH	50.2	18	1.63	3.76×10^{-4}

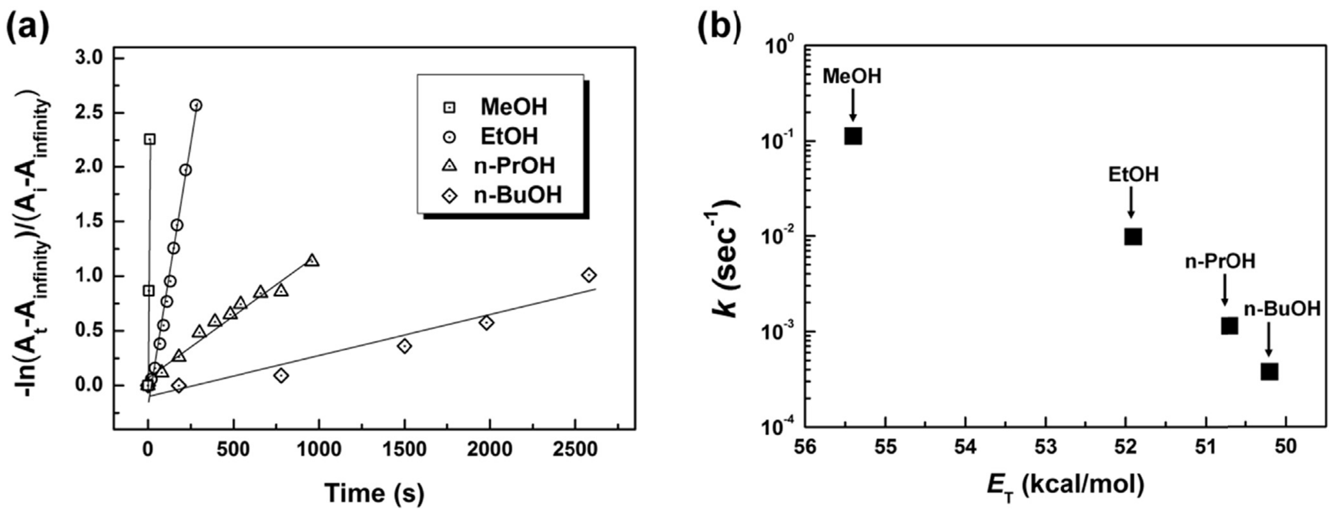

Fig. 7. (a) First-order kinetic plots of $CH_3NH_3PbI_3$ in the presence of MeOH, EtOH, n-PrOH, and n-BuOH and (b) plots showing relationship between polarity of alcohols and reaction rate.

absorbance at 420 nm after full conversion and first-order rate constant, respectively [11]. During the color changing reaction, the kinetic analysis predicts the logarithm of the difference between A_∞ and A_t at time t to be linear with time, where the slopes provide the color change rate constant, k. First-order plots according to Eq (3) are presented in Fig. 7a. The first reaction rate constants for MeOH, EtOH, n-PrOH, and n-BuOH were determined as $k = 1.13 \times 10^{-1}$, 9.78×10^{-3}, 1.14×10^{-3}, and 3.76×10^{-4} sec^{-1}, respectively. These results indicate that the hydrogen bonding interaction occurs more readily in the following order: MeOH $\gg$ EtOH > n-PrOH > n-BuOH, which is in a good accordance with the order of their polarity values as plotted in Fig. 7b.

The reaction rate greatly decreases as alkyl chain length or number of hydrocarbon attached to oxygen atom increases from 1 (MeOH) to 4 (n-BuOH). Considering that difference in electronegativity (χ) between carbon (2.55) and oxygen (3.44) in a C—O bond plays a crucial role in generating polarity of the alcohols, this observation means that longer alkyl chain will weaken the negative charge of the oxygen atom due to the increased portion of non-polar hydrocarbons.

Molecular electrostatic potential (MEP) surface is a useful protocol to interpret and compare relative reactivity or reactive sites for hydrogen bonding interactions, electrophilic/nucleophilic reactions, and molecular cluster and crystal behavior by mapping electrostatic potential on the molecule surfaces [12]. Fig. 1b presents MEPs of MeOH, EtOH, n-PrOH, and n-BuOH, where red and blue colors indicate electron-rich regions with partial negative charge and electron-deficient regions with partial positive charge, while yellow and green colors indicate slightly electron-rich and neutral regions, respectively.

MEPs in Fig. 1b shows that electron-deficient sites of alcohols are located over oxygen atoms of hydroxyl groups and electron-rich sites are present over hydrogen atoms attached to hydroxyl group. More importantly, enlarged neutral portion in the alcohol molecules is observed with increased alkyl chain lengths due to the increased portion of non-polar hydrocarbons. Decreased negative potential on the oxygen atom, therefore, results in weaker hydrogen bonds between polar units (CH3NH3$^+$ and I$^-$) in $CH_3NH_3PbI_3$ and OH in alcohols and subsequently delays intermolecular interaction rate and color changes. Moreover, both linear steric hindrance and hydrophobic effects from longer alkyl chain also hamper the hydrogen bonding interaction and lower the interaction rate.

4. Conclusions

In conclusion, we developed a simple but very sensitive chemosensor for distinguishing polarity of molecules using highly chromogenic $CH_3NH_3PbI_3$ perovskite functional dye. Polar alcohols were clearly detected from color changes from dark brown to yellow which was visible with naked eyes, and moreover difference in polarity of alcohols was also precisely observed from color change time or reaction rate. Based on these results we found that the hydrogen bonding interaction between perovskite dye and alcohols is the driving force for the polarity detection and the strength of the hydrogen bonds had a significant effect on the practical recognition of the degrees of polarity.

Acknowledgements

This research was supported by Basic Science Research Program through the National Research Foundation (NRF) funded by the Ministry of Science, ICT and Future Planning (2015R1C1A1A01053241). This work was supported by the National Research Foundation of Korea (NRF) grant funded by the Korea government (MSIP) (No. 2014002985).

References

[1] (a) Vance DH, Czarnik AW. Real-time assay of inorganic pyrophosphatase using a high-affinity chelation-enhanced fluorescence chemosensor. J Am Chem Soc 1994;116:9397–8.
(b) Lee HN, Xu Z, Kim SK, Swamy KMK, Kim Y, Kim S-J, et al. Pyrophosphate-selective fluorescent chemosensor at physiological pH: formation of a unique excimer upon addition of pyrophosphate. J Am Chem Soc 2007;129:3828–9.
(c) Park S, Kim W, Swamy KMK, Lee HY, Jung JY, Kim G, et al. Rhodamine hydrazone derivatives bearing thiophene group as fluorescent chemosensors for Hg2+. Dyes Pigments 2013;99:323–8.
(d) Jung J, Han SJ, Chun J, Lee C, Yoon J. New thiazolothiazole derivatives as fluorescent chemosensors for Cr3+ and Al3+. Dye Pigments 2012;94:423–6.
(e) Kimura M, Horai T, Hanabusa K, Shirai H. Fluorescence chemosensor for metal ions using conjugated polymers. Adv Mater 1998;10:459–62.
(f) Basabe-Desmonts L, Reinhoudt DN, Crego-Calama M. Design of fluorescent materials for chemical sensing. Chem Soc Rev 2007;36:993–1017.

[2] (a) Yoon J, Chae S, Kim J-M. Colorimetric sensors for volatile organic compounds (VOCs) based on conjugated polymer-embedded electrospun fibers. J Am Chem Soc 2007;129:3038–9.
(b) Lee JY, Kim SK, Jung JH, Kim JS. Bifunctional fluorescent calix[4]arene chemosensor for both a cation and an anion. J Org Chem 2005;70:1463–6.
(c) Green AM, Naughton HR, Nealy ZB, Pike RD, Abelt CJ. Carbonyl-twisted 6-acyl-2-dialkylaminonaphthalenes as solvent acidity sensors. J Org Chem 2013;78:1784–9.
(d) Zhang H, Feng L, Liu B, Tong C, Lü C. Conjugation of PPV functionalized mesoporous silica nanoparticles with graphene oxide for facile and sensitive fluorescence detection of TNT in water through FRET. Dyes Pigments 2014;101:122–9.

[3] (a) Telore RD, Sekar N. Carbazole-containing pushepull chromophore with viscosity and polarity sensitive emissions: synthesis and photophysical properties. Dyes Pigments 2016;129:1–8.
(b) Onoda M, Uchiyama S, Ohwada T. Fluorogenic ion sensing system working in water, based on stimulus-responsive copolymers incorporating a polarity-sensitive fluorophore. Macromolecules 2007;40:9651–7.
(c) Signore G, Nifosì R, Albertazzi L, Storti B, Bizzarri R. Polarity-sensitive coumarins tailored to live cell imaging. J Am Chem Soc 2010;132:1276–88.

[4] Park N-G. Perovskite solar cells: an emerging photovoltaic technology. Mater Today 2015;18:65–72.

[5] Niu G, Guo X, Wang L. Review of recent progress in chemical stability of perovskite solar cells. J Mater Chem A 2015;3:8970–80.

[6] Jeon NJ, Noh JH, Kim YC, Yang WS, Ryu SC, Seok SI. Solvent engineering for high-performance inorganic–organic hybrid perovskite solar cells. Nat Mater 2014;13:897–903.

[7] Liu M, Johnston MB, Snaith HJ. Efficient planar heterojunction perovskite solar cells by vapour deposition. Nature 2013;501:395–8.

[8] Jiang C, Lim SL, Goh WP, Wei FX, Zhang J. Improvement of $CH_3NH_3PbI_3$ formation for efficient and better reproducible mesoscopic perovskite solar cells. ACS Appl Mater Interfaces 2015;7:24726–32.

[9] Manser JS, Saidaminov MI, Christians JA, Bakr OM, Kamat PV. Making and breaking of lead halide perovskites. Acc Chem Res 2016;49:330–8.

[10] Dong X, Fang X, Lv M, Lin B, Zhang S, Ding J, et al. Improvement of the humidity stability of organic–inorganic perovskite solar cells using ultrathin Al_2O_3 layers prepared by atomic layer deposition. J Mater Chem A 2015;3:5360–7.

[11] Wang Y, Kim S-H. Colorimetric chemodosimeter for cyanide detection based on spiropyran derivative and its thermodynamic studies. Dyes Pigments 2014;102:228–33.

[12] Ou YH, Chang M, Chen YS. A QSPR study on the solvent-induced frequency shifts of acetone and dimethyl sulfoxide in organic solvents. Spectrochim Acta A 2016;162:109–14.